13th World Conference on Earthquake Engineering
Vancouver, B.C., Canada
August 1-6, 2004
Paper No. 746

RELIABILITY-BASED SEISMIC DESIGN OF NEAR-FAULT BRIDGE STRUCTURES IN TAIWAN

Chiun-lin WU[1], Chu-Chieh Jay LIN[2] and Chin-Hsiung LOH[3]

SUMMARY

This study investigates simply supported bridge systems with nonlinear isolators subjected to perfectly correlated equivalent pulse-like motions with arrival time delay at two separate piers. The important characteristics of equivalent pulse motion, such as pulse period, permanent fault offset and peak horizontal velocity, are determined from probabilistic seismic hazard analysis. The proposed approach provides convenient response estimations of bridges subjected to near-fault excitations, which are useful for preliminary design of new bridges and for a rapid performance evaluation of existing bridges. Finally, a recommended procedure for planning and design of near-fault/fault-crossing bridges is provided to ensure satisfactory level of safety of fault-crossing bridges and availability of alternative transportation route between cities in case of bridge failure.

INTRODUCTION

The Chi-Chi (Taiwan) earthquake of September 21 1999 (local time) caused widespread damage to highway bridges in the central part of Taiwan, especially those crossing directly over or close to the Chelungpu fault experienced moderate-to-major damage. Since then, researchers in Taiwan have been conducting extensive investigations on near-fault and fault-crossing bridges to mitigate life and economic loss due to major probable events in the future. In this study, probabilistic seismic hazard analysis (PSHA) was conducted with empirical characterization of near-fault earthquakes to generate artificial equivalent pulse motions. These pulse motions were then used in nonlinear time history analyses for simply supported bridge systems, in which effects of dynamic directivity pulse and wave arrival delay between two adjacent piers were included. Return period of major events were considered in response computation to establish a tentative methodology framework for performance-based seismic evaluation of bridge structures. A recommended planning and design procedure is given for special cases of fault-crossing bridges. It is mentioned that the proposed design check method can only serve as an additional tool for bridge response estimation whenever near-fault pulse-type of motions are of concern, whereas a

[1] Postdoctoral Research Associate, Center for Earthquake Engineering Research, National Taiwan University, Taiwan, ROC. Email: clwu@ncree.gov.tw
[2] Division Chief, Taiwan Construction Research Institute, Taiwan, ROC. Email: linjay@tcri.org.tw
[3] Professor, Department of Civil Engineering, National Taiwan University, Taiwan, ROC. Email: lohc@ncree.gov.tw

conventional code-specified procedure should be followed as well to yield bridge response under ordinary broadband excitations.

MODELING OF HIGHWAY BRIDGE WITH SIMPLY SUPPORTED GIRDER

A simply supported bridge system is schematically shown in Figure 1(a). The superstructure is supported on elastomeric bearing pads on top of drop bent cap. It is favorable that in case of a major event damage occurs only in bridge isolators and other major components remain elastic; nonlinearity is thus assumed to exist only in the bearing pads in the subsequent analysis. A free body diagram of the simplified bridge system is shown in Figure 1(b). The equation of motion for the lumped mass mathematical model can be expressed in the following matrix form:

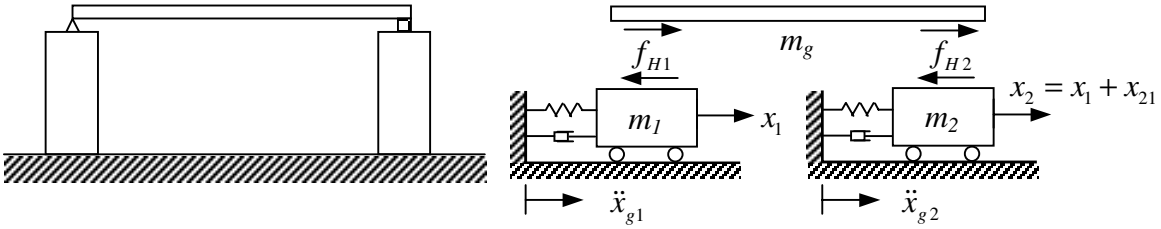

(a) (b)

Figure 1. Single span highway bridge system: (a) schematic plot, (b) simplified analytical model.

$$\begin{bmatrix} 1+a & 0 \\ b & b \end{bmatrix}\begin{Bmatrix} \ddot{x}_1 \\ \ddot{x}_{21} \end{Bmatrix}+\begin{bmatrix} 2\xi_1\omega_1 & -2\gamma\xi_1\omega_1 \\ 2b\xi_2\omega_2 & 2b\xi_2\omega_2(1+\alpha) \end{bmatrix}\begin{Bmatrix} \dot{x}_1 \\ \dot{x}_{21} \end{Bmatrix}+\begin{bmatrix} \omega_1^2 & -\rho\alpha_b\omega_1^2 \\ b\omega_2^2 & b\omega_2^2(1+\beta\alpha_b) \end{bmatrix}\begin{Bmatrix} x_1 \\ x_{21} \end{Bmatrix}$$
$$+\begin{Bmatrix} -b\omega_2^2\beta(1-\alpha_b) \\ b\omega_2^2\beta(1-\alpha_b) \end{Bmatrix} z=\begin{bmatrix} 2\xi_1\omega_1 & 0 \\ 0 & 2b\xi_2\omega_2 \end{bmatrix}\begin{Bmatrix} \dot{x}_{g1} \\ \dot{x}_{g2} \end{Bmatrix}+\begin{bmatrix} \omega_1^2 & 0 \\ 0 & b\omega_2^2 \end{bmatrix}\begin{Bmatrix} x_{g1} \\ x_{g2} \end{Bmatrix} \quad (1)$$

and,

$$2\xi_1\omega_1=\frac{c_1}{m_1},\ 2\xi_2\omega_2=\frac{c_2}{m_2},\ \omega_1^2=\frac{k_1}{m_1},\ \omega_2^2=\frac{k_2}{m_2},$$
$$a=\frac{m_g}{m_1},\ b=\frac{m_2}{m_1},\ c_3=\alpha c_2=\gamma c_1,\ k_3=\beta k_2=\rho k_1$$

where x_1 = absolute displacement of pier 1; x_{21} = relative displacement between girder and pier 2; x_{g1} and x_{g2} = ground displacement at the foundation of pier 1 and pier 2, respectively; dot indicates time derivative; m_1, m_2 and m_g = mass of pier 1, pier 2 and girder, respectively; k_1, k_2 and k_3 = stiffness of pier 1, pier 2 and isolator, respectively; c_1, c_2 and c_3 = viscous damping coefficient of pier 1, pier 2 and isolator, respectively; ω_i = circular frequency; ξ_i = damping ratio critical (i = 1, 2). The hysteretic behavior of the bearing pad takes the form:

$$f_s=k_3\alpha_b x_{21}+k_3(1-\alpha_b)z \quad (2)$$

where f_s is restoring force, and auxiliary state variable z describes the hysteretic path in a bilinear form as follows [1]:

$$\dot{z} = \frac{1}{\eta}\left\{ A \cdot \dot{x}_{21} - \nu \cdot \beta_b \cdot \left|\dot{x}_{21}\right| \cdot \left|z\right|^{n-1} \cdot z - \nu \cdot \gamma_b \cdot \dot{x}_{21} \cdot \left|z\right|^{n} \right\} \tag{3}$$

where $A, \beta_b, \gamma_b, \nu, \eta$ and n are shape controlling parameters (e.g., $A = \nu = \eta = 1$ corresponds to non-degrading systems); α_b = post-to-preyield stiffness ratio of the bearing pad. A typical hysteretic loop of the lead rubber bearing is shown in Figure 2. In passing, it is noted that Jao [2] reported the simple 2-DOF lumped-mass model provided satisfactory approximation to a sophisticated FEM model. This study, based on Jao, thus made further modifications to include consideration of two input motions at two separate piers.

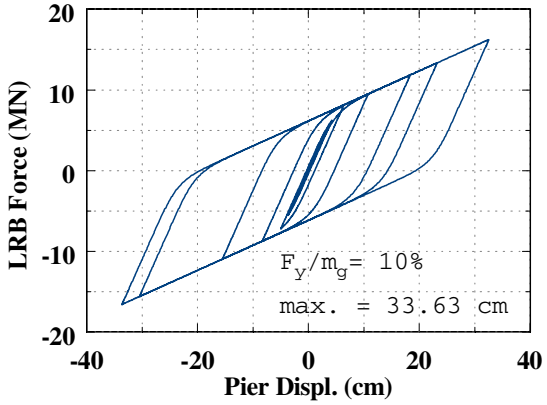

Figure 2. A typical bilinear hysteretic loop of lead rubber bearing.

EMPIRICAL CHARACTERIZATION OF NEAR-FAULT GROUND MOTIONS

How the seismic waves attenuate when travelling away from the ruptured fault generally depends on faulting mechanism of the rupture, geological and topographical conditions along the propagating path. As such, the definition of "near fault" will defer from country to country, or more precisely in a scientific term, seismic-zone dependent. In the 2001 seismic design code for highway bridges in Taiwan, the near-fault zone is defined to be within a distance of about 5~11 km from an active fault trace. It is well known that near-fault ground motion may contain distinct forward directivity pulse and fling step motion, which can cause severe damage to engineering structures. This pulse-type of motion is typically characterized by large amplitude at intermediate to long periods and short duration [5]. When the geometric conditions for forward directivity are satisfied, the effects of forward directivity may not occur. This is because asperity and ratio of rupture velocity to shear wave velocity are the additional affecting factors to realize forward directivity. Worldwide field observations show that most near-fault ground motions are of narrowband nature according Stewart et al. [6]; the same has been observed in the 1999 Chi-Chi earthquake as shown in Figure 3. Taking the northern branch of the Chelungpu fault as an example, Figure 4 shows that the two orthogonal principal axes in the vicinity of station TCU068 coincide with fault normal and fault parallel directions, i.e. approximately the northeastern direction. Such empirical rules provide a promising method to construct near-fault pulse type of motions. Another very important aspect is pointed out by the red dotted lines in Figure 4; i.e., velocity and displacement will reach their peak values at the same time and this should be followed strictly when bi-directional excitation is under consideration to ensure design on a safe side. Since to this date near-fault recordings are still quite limited, equivalent pulse motions thus become an appropriate alternative to be used in dynamic analysis whenever near-fault seismic risk is a

concern. Available from the literature are rectangular, triangular, and sinusoidal equivalent pulse motions, among which the sinusoidal pulse motion such as those shown in Figure 5 was adopted in this study in view that it better represents field records in wave form and is also capable of capturing the salient natures of rupture directivity. Field observations reveal that, for most cases, number of cycles of pulses range from 0.5 to 2 cycles, however Stewart et al. [6] found that one full cycle would be a good general value to use in seismic evaluation, which is also followed in this study. To construct equivalent pulse of motions, empirical formulae are available from the literature (Table 1). Comparisons are made in Figures 6-9. It appears that Rodriguez-Marek [7] provides better match with peak horizontal velocities observed in the 1999 Chi-Chi earthquake, most likely because a broader database was used by Rodriguez-Marek for his statistical study. Rodriguez-Marek attenuation form was therefore adopted in PSHA. Figure 8 shows that the average fault displacement of the 1999 Chi-Chi earthquake is higher than the average curve predicted by Wells-Coppersmith empirical formula. On the other hand, it is difficult to make judgment which empirical formula for pulse period is more appropriate at the present stage. Figures 7 and 9 indicate that although pulse period does have a moderate correlation with magnitude and peak horizontal velocity, applications in engineering practice at the present stage may not yield very accurate analysis results due to modeling uncertainty. This may result from complexity of the source mechanism of the 1999 Chi-Chi earthquake. Logic tree or worst scenario could be a good choice in such cases. However, empirical formulas can be improved as more near-fault records are collected from around the world in the future and more knowledge is obtained of near-fault seismic characteristics.

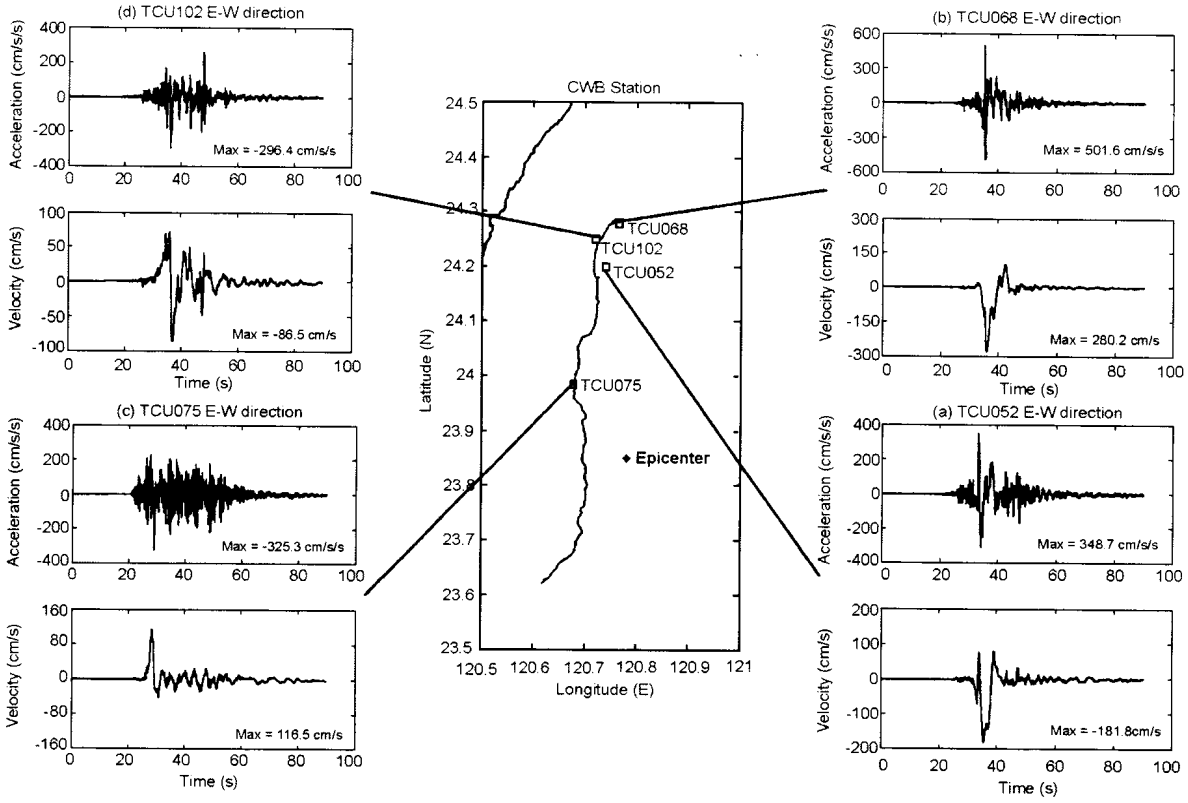

Figure 3. Ground acceleration and velocity time histories from 4 stations along Chelungpu fault (after Lee and Loh [3]).

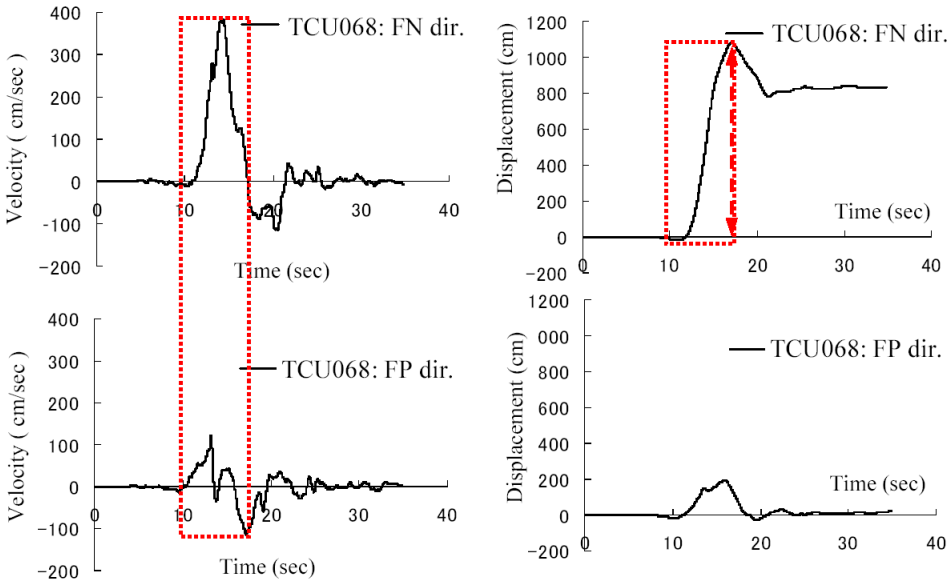

Figure 4. Baseline-corrected TCU068 velocity and displacement time histories at the Shihkang Elementary School along the fault-normal and fault-parallel directions (after Hisada [4] with modifications).

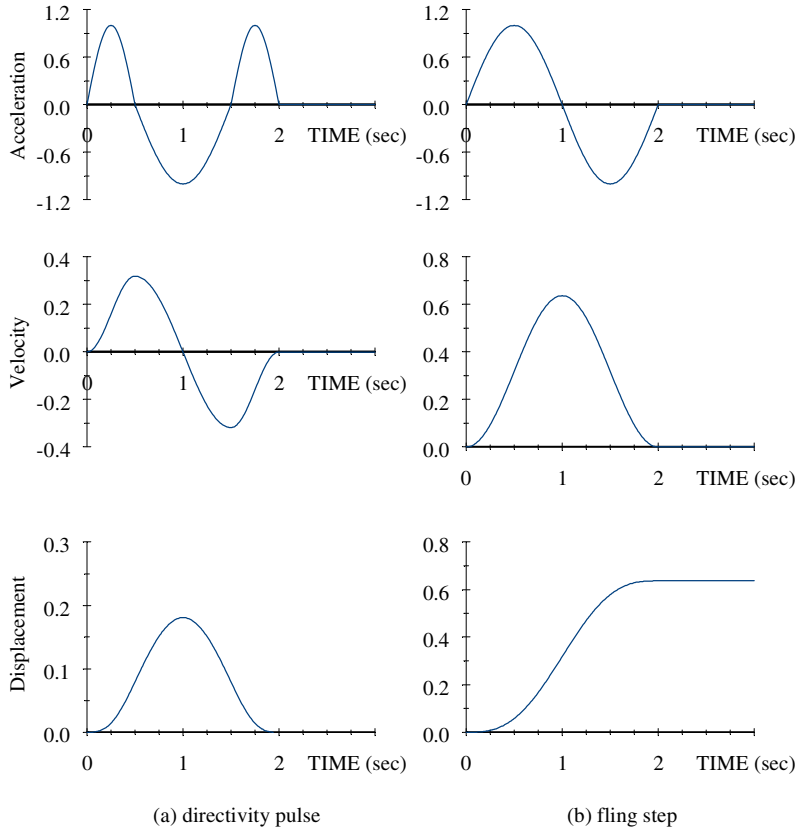

Figure 5. Sinusoidal equivalent pulse motions: (a) directivity and, (b) fling step pulse of motions.

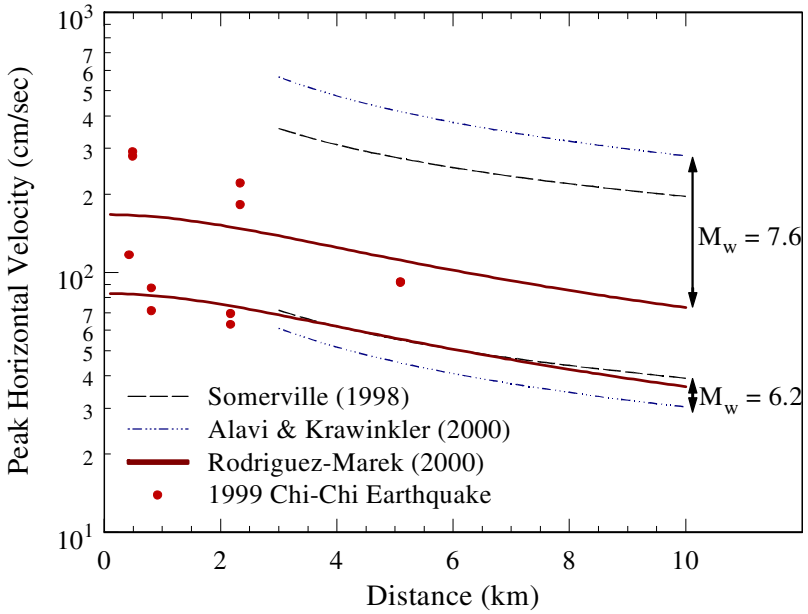

Figure 6. Comparison of *PHV* attenuation relationships with the 1999 Chi-Chi earthquake records.

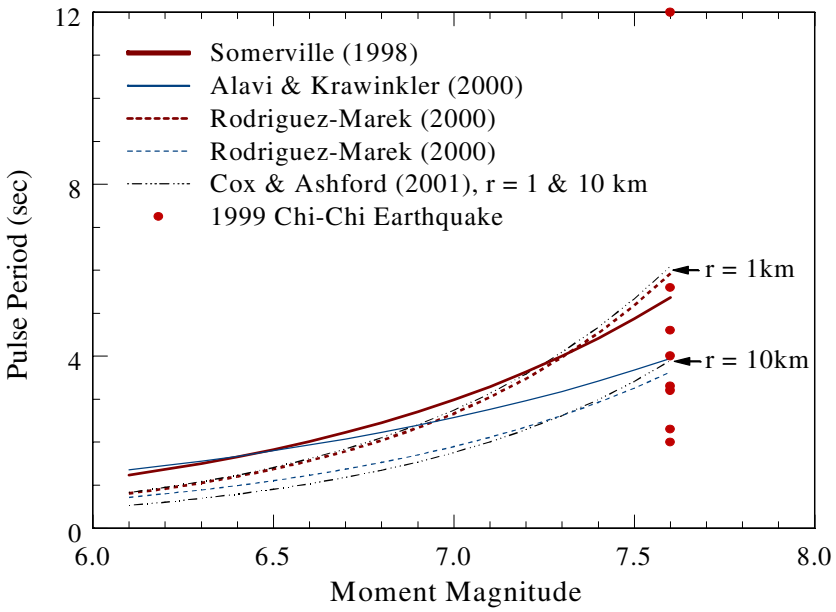

Figure 7. Comparison of empirical formulas for pulse period (T_v, $T_{v\text{-}p}$) with the 1999 Chi-Chi earthquake records.

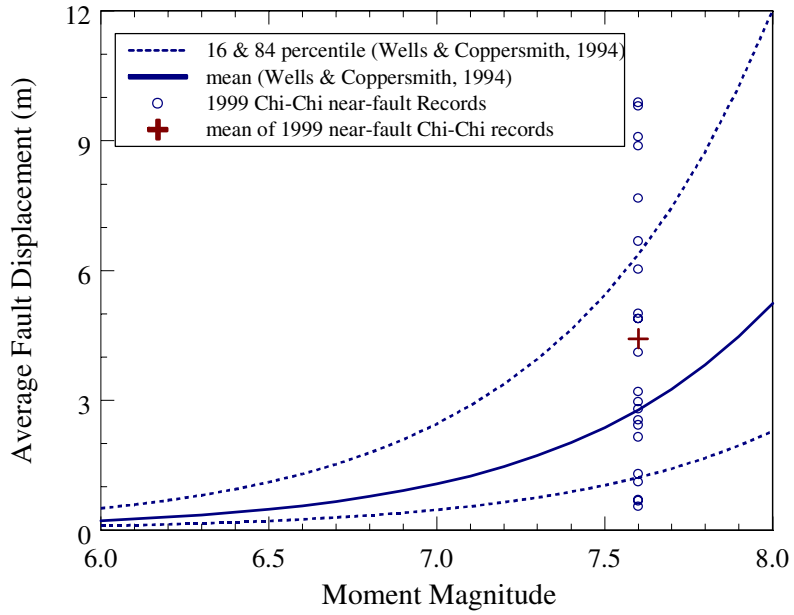

Figure 8. Comparison of empirical formula for average fault displacement with the 1999 Chi-Chi earthquake records.

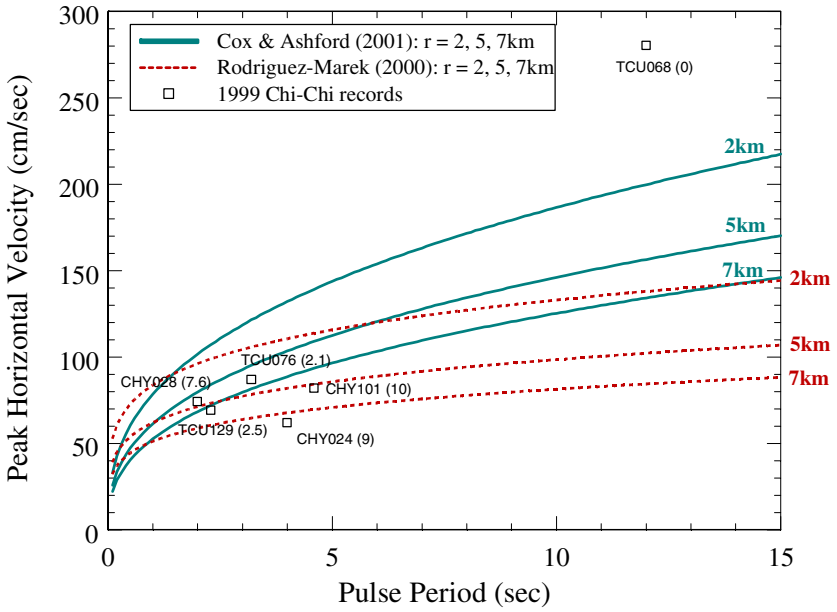

Figure 9. Comparison of empirical *PHV-*T_v equations with the 1999 Chi-Chi earthquake records. (The station code is indicated next to symbol ; closest distance to the vertical projection of the rupture surface in units of km is enclosed in parentheses.)

Table 1. Empirical formulas for near-fault pulse-type of motions.

Reference	Pulse Period (sec)	Peak Horizontal Velocity (cm/sec)
Somerville (1998)	$\log(T_v) = -2.5 + 0.425 \cdot M_w$	$\ln(PHV) = -2.31 + 1.15 \cdot M_w - 0.5 \cdot \ln(r)$
Alavi & Krawinkler (2000)	$\log(T_{v\text{-}p}) = -1.76 + 0.31 \cdot M_w$	$\ln(PHV) = -5.11 + 1.59 \cdot M_w - 0.58 \cdot \ln(r)$
Rodriguez (2000)	$\ln(T_v) = -8.33 + 1.33 \cdot M_w + \varepsilon$; $\varepsilon = 0.54$ $\ln(T_{v\text{-}p}) = -6.92 + 1.08 \cdot M_w + \varepsilon$; $\varepsilon = 0.66$	$\ln(PHV) = -2.44 + 0.5 \cdot M_w - 0.41 \cdot \ln(r^2 + 3.93^2)$
Cox & Ashford (2001)	$\log(T_{v\text{-}p}) = -3.579 + 0.5770 \cdot M_w - 0.02153 \cdot r$	

T_v = period of the largest cycle of motion (sec); M_w = moment magnitude; ε = error term.
$T_{v\text{-}p}$ = predominant period in a velocity response spectrum plot (sec).
r = distance to rupture surface (km); PHV = peak horizontal velocity (cm/sec).

Table 2. Cefficients of seven active faults in Taiwan.

Fault Name	Faulting Mechanism	Fault Length (km)	Fault Width (km)	M_o	M_u	b-value	Slip Rate (cm/yr)	Annual Occurrence Rate
Shintan Fault	reverse-slip	15	15	4.5	7.20	0.78119	0.5	0.0202
Tuntzuchiao Fault	right-lateral	14	14	4.5	7.10	0.78119	0.5	0.0188
Chelungpu Fault	reverse-slip	90	58.5	4.5	7.52	0.78119	0.6	0.1203
Meishan Fault	right-lateral	13	13	4.5	7.10	1.08596	0.5	0.0479
Tachienshan and Chukou Fault	reverse-slip	92	23	4.5	7.31	1.08596	0.5	0.1901
Hsinhua Fault	right-lateral	6	6	4.5	6.50	1.08596	0.5	0.0177
Huatung Longitudinal Valley	reverse-slip	98	23	4.5	7.28	1.01132	0.5	0.6585

M_0 = minimum magnitude; M_u = maximum magnitude.

PROBABILISTIC SEISMIC HAZARD ANALYSIS

Probabilistic seismic hazard analyses, following the general procedure of Cornell [11] and Berrill [12], were performed against peak horizontal velocity and average ground offset, which are required for simulating equivalent pulse motions. The CGS-defined 12 active faults of Taiwan [13] were re-grouped into 7 faults, considered as potential sources for characteristic earthquakes (Figure 10). Important coefficients of the 7 active faults are given in Table 2. In addition, distributed earthquakes were assumed in background source zones. To perform PSHA, information on distribution of seismogenic zones, source model, rupture length-magnitude relationship, offset-magnitude relationship, maximum and minimum magnitudes, magnitude recurrence model, distribution of focal depth, empirical attenuation equation is required. Values of the seismic parameters used for analysis in this study can be referred to Loh and Huang [14]. In Figure 11, average offset reaches an upper bound corresponding to the maximum magnitude earthquake likely to occur on the fault. In Figure 13(a), scenario earthquakes are assumed to generate from the Chelungpu fault. Three hazard curves are given, corresponding to 2, 5, and 7km away from the fault trace, and these hazard curves, when combined with T_v-PHV relationships (Figure 13(b)), enable relating pulse period to the annual probability of exceedance. It is observed from Figure 11 that,

for the Chelungpu fault, ground offset has been underestimated using the empirical formula of Berrill. The same has been observed for average fault displacement in Figure 8. Further investigations on this issue are strongly recommended because such underestimation may occur to other active faults in Taiwan as well. The problem should be resolved before reliable prediction can be expected.

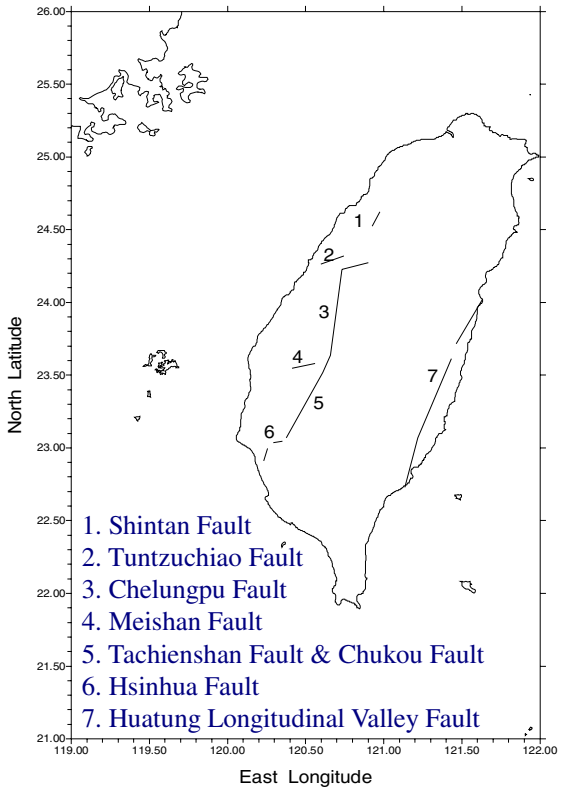

Figure 10. Seven active faults in the island of Taiwan.

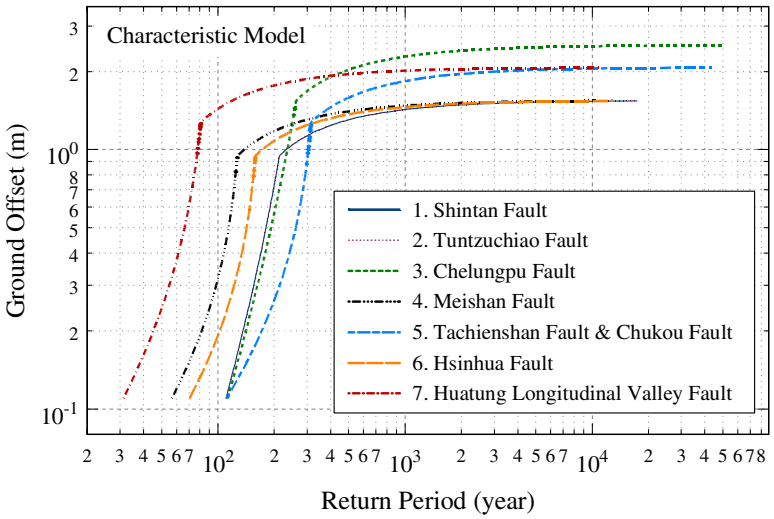

Figure 11. Offset-return period relationship.

DYNAMIC TIME HISTORY ANALYSIS OF SIMPLY SUPPORTED BRIDGE

According to Hwang et al. [15], the following characteristics are assumed of the lead rubber bearing pad:

$$\alpha_b = 0.15,\ \beta = k_3 / k_2 = 0.5,\ k_3 = F_y / D_y,\ F_y = 0.1 m_g,\ \beta_b = \gamma_b = 1/\left(2D_y^{\ n}\right),\ n = 3$$

A 0.1-sec delay time is assumed to input motions at two adjacent piers. The bridge is then subjected to equivalent pulse motions of various periods. Three demand curves are constructed for bridges with fundamental periods of 0.5, 0.7 and 1.0 sec as shown in Figure 12, which can be used to determine the size of drop bent cap to prevent superstructure from dislocation. In addition, a tentative procedure to determine isolator ductility demands at multiple hazard levels is proposed (Figure 13). For a specified hazard level, peak velocity and pulse period can be estimated as aforementioned, and then ductility and deformation of the bearing pad are thus readily determined from the demand curves provided in Figure 13(c)-(d), where pulse period is normalized by the fundamental period of the bridge system. These demand curves help practicing engineers select appropriate isolators that satisfy design criteria.

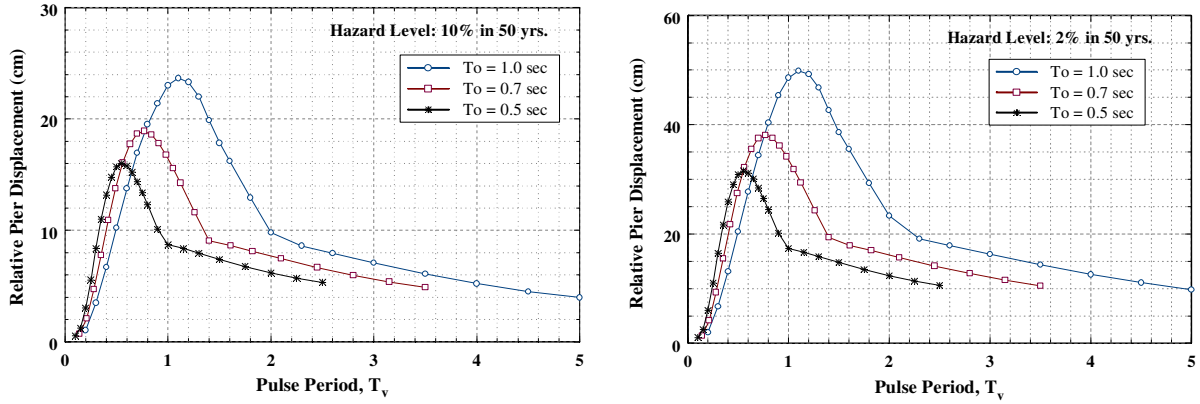

Figure 12. Displacement demands for general bridge stocks: hazard level 10% (left), and 2% (right) in 50 yrs.

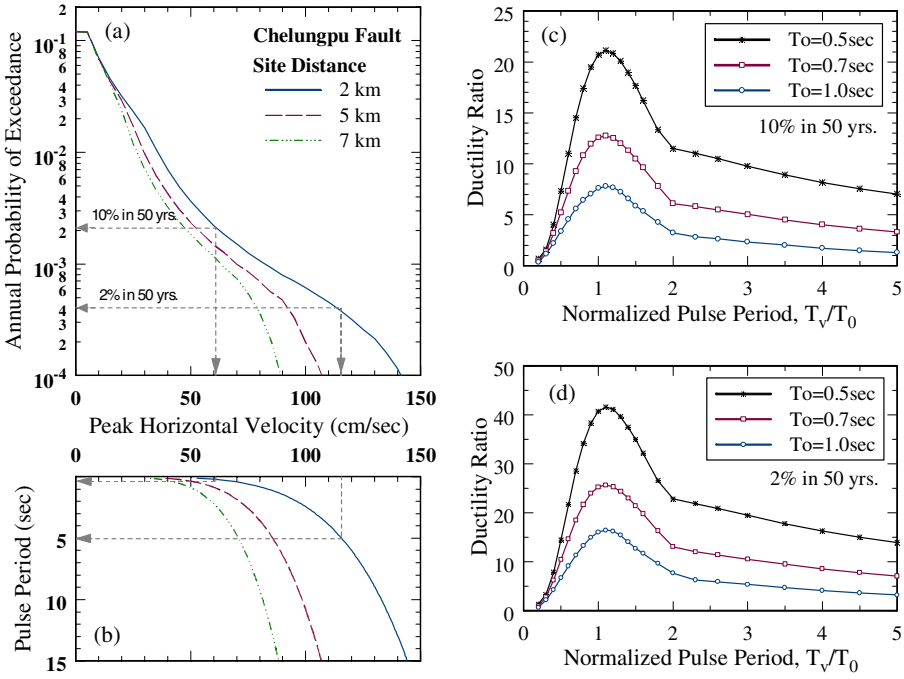

Figure 13. Tentative procedure to determine isolator ductility demands at duel hazard levels.

ISSUES ON PLANNING AND DESIGN OF FAULT-CROSSING BRIDGES

It may be unlikely in special cases to avoid severe structural damage such as bridge collapse and column tilting caused by combined effects of dynamic ground shaking and static displacement offset during a rare earthquake event. The consequential damage such as loss of lives, properties, and tremendous economic impact, however, can be reduced as much as possible if the planning and design procedure of fault-crossing bridges comply with appropriate guidelines. Following the same engineering philosophy of earthquake-prone countries, the current practice of Taiwan's Directorate General of Highways (DGH) and Taiwan Area National Expressway Engineering Bureau (TANEEB) under the Ministry of Transportation and Communication (MOTC) aims to avoid building bridges across known active faults in the stage of route planning, but still there are possibilities that this goal can not be fully accomplished since Taiwan is among the most densely populated countries in the world. As such, possible alternatives (e.g., building embankment over the active fault) are always considered as a priority. If unfortunately there are no feasible alternatives, then the planning and design procedure shown in Figure 14 should be followed closely when building a bridge over active fault(s) on the planned route. Major elements in the flowchart are briefly explained as follows:

Technical Advisory Panel

A Technical Advisory Panel (TAP) should be formed to review technical issues and provide expert recommendations on demand and capacity assessment of the fault-crossing bridge structure in severe seismic events. The TAP committee, selected by the owner, should consist of at least 5 persons including experts on bridge engineering, earthquake engineering and geology (professor, professional engineer and geologist). TAP committee is responsible for providing opinions and suggestions on combined effects of strong ground shaking and surface fault rupture, fault displacement hazard, guidance for selection of structural type and bridge isolation/control system, construction details, etc. to the owner and the design team.Type text immediately below sub-subheadings

Bridge Site Geological Probing

It is essential to conduct comprehensive geological probing of the bridge site and seismogenic data collection surrounding active faults. Engineering consultants should perform detailed geotechnical and geological studies (e.g., past fault rupture history, downhole boring log data, etc.) Trenching study and surface rupture evidence may reveal more historical information on fault ruptures in the vicinity of the planned bridge site and field investigation findings can be taken into consideration of the deterministic or probabilistic hazard analysis.

Hazard Mitigation Plan

It is impractical to design a rupture-crossing bridge free from damages during a rare earthquake event, such as bridge dislocation, column tilting, etc. and occasionally collapse prevention may not be guaranteed. In such cases, local hazard mitigation plan must come along with the analysis-design-construction project of the fault-crossing bridge. The emergency response plan should include fast repairing method, substitute route, and construction of emergency overpass.

Near Fault Effect / Fault Displacement Offset

In the framework of performance-based design methodology, probabilistic seismic hazard analyses should be carried out on critical design parameters, including near-fault peak horizontal velocity, dominant pulse period and permanent ground offset, etc. Earthquake recordings nearby the bridge site are also desirable to be used for dynamic analysis.

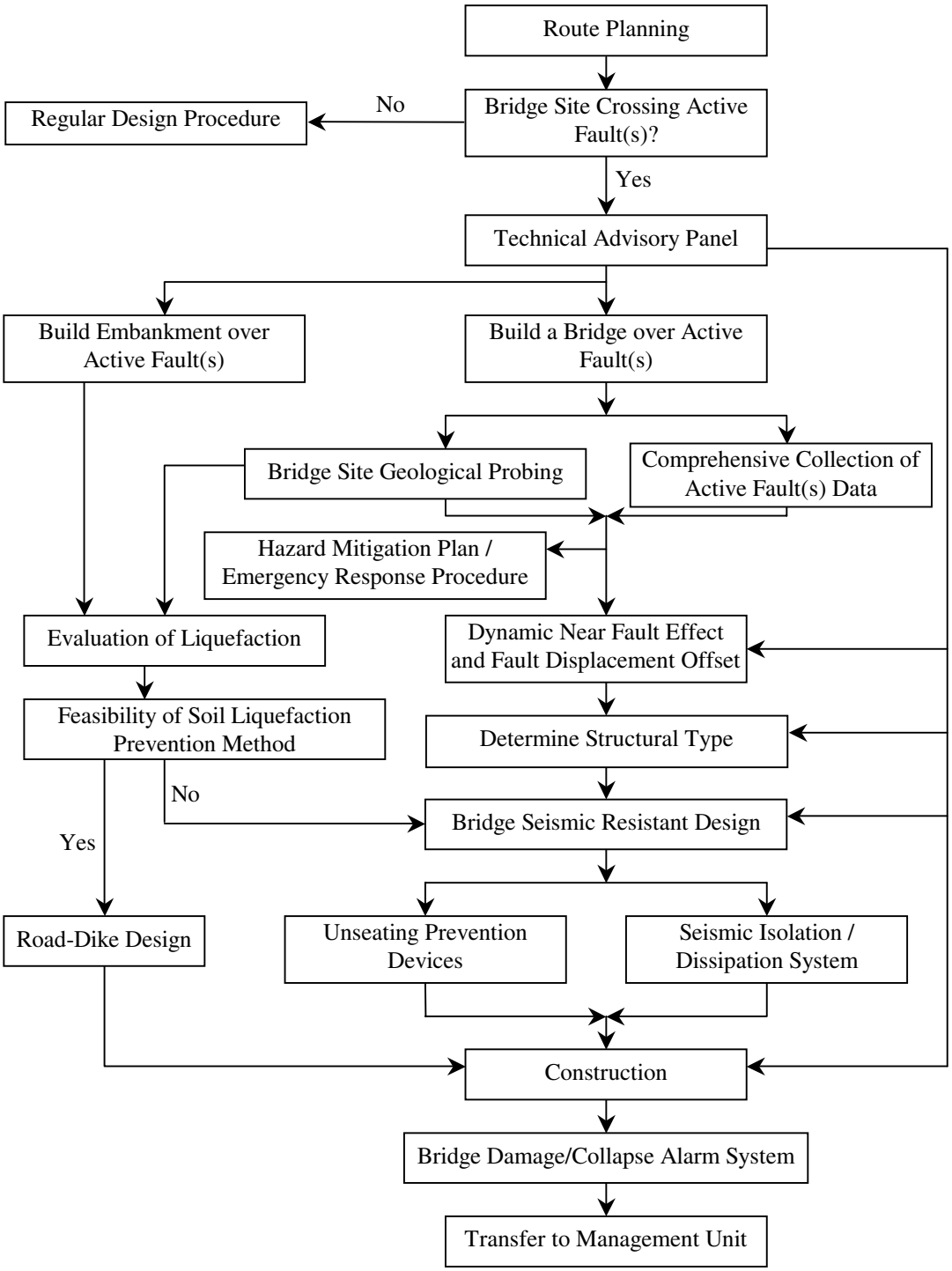

Figure 14. Flowchart illustrating recommended planning and design procedure for fault-crossing bridges in Taiwan.

Selection of Structural Type

There are several options for the structural types of fault-crossing bridges, including: (1) simply supported bridge, (2) steel bridge, (3) long-span bridge, (4) stand-alone rigid frame bridge, (5) cantilever bridge, and (6) multi-span continuous bridge. However, every one of them has its own drawbacks and limitations in undertaking maximum possible surface rupture as well as resisting strong ground acceleration. The pros and cons of each bridge type need to be carefully reviewed in a case-by-case basis. Higher degree of redundancy is always considered a rule of thumb in design of such bridges.

Soil Liquefaction Evaluation

Soil liquefaction is a common phenomenon for areas with higher water table levels during strong earthquake shaking. During the 1999 Chi-Chi earthquake, soil liquefaction and ground settlement causing serious damage to bridges had been reported in central Taiwan. The evaluation of liquefaction potential using subsurface soil properties obtained from SPT and observations from past earthquakes should be undertaken in the design stage. Soil liquefaction potential needs to be quantitatively characterized and prevention measures and soil improvement methods should be provided.

Bridge Seismic Resistant Design

Bridge seismic resistant design with consideration of isolation/dissipation systems is desirable. Rational analysis methods such as nonlinear time history analysis are highly recommended. Considerations should also be given to the choice of unseating prevention devices such as stop-blocks, seismic resistant rods and so on.

Bridge Collapse Alarm System

After the bridge construction is complete and opened to traffic, a real-time bridge collapse alarm system is favorable in order to warn in-moving vehicles of bridge collapse occurrences to save lives or minimize loss of lives. The alarm system consists of alarms and measuring instruments such as inclinometer, load cell, etc.

CONCLUSIONS

A tentative performance-based procedure for seismic evaluation of bridge structures subjected to near-fault pulse excitations are proposed in this study. In addition to conventional response check under ordinary broadband earthquake motions, the proposed method can serve as a secondary response check of simply supported bridges subjected to near-fault pulse-type of motions, which are useful for preliminary design of new bridges and for a rapid performance evaluation of existing bridges. The proposed model is able to take into account response amplification effects caused by wave arrival delay between piers. This study presents a convenient approach to estimate responses of bridges when near-fault effects are of concerns.

ACKNOWLEDGEMENTS

The financial support for this study from the Public Construction Commission, Executive Yuan of Taiwan is gratefully acknowledged. The authors would like to give special thanks to Mr. Yung-Jui Huang of NCREE for carrying out numerical calculation in PSHA. All opinions expressed in this paper are solely those of the authors, and do not necessarily represent those of the sponsor.

REFERENCES

1. Wen YK. "Method for random vibration of hysteretic systems." Journal of Engineering Mechanics Division, ASCE, 1976; **102**: 249-263.
2. Jao SA. "Response analysis of isolated bridge: consideration of near-fault and far-field earthquake ground motions." Master Thesis, Department of Civil Engineering, National Taiwan University, Taipei, Taiwan, (in Chinese), 2001; adviser: Loh CH.
3. Lee GC, Loh CH, Editors. "The Chi-Chi, Taiwan earthquake of September 21, 1999: reconnaissance report." Multidisciplinary Center for Earthquake Engineering Research, University at Buffalo, Technical Report MCEER-00-0003, April 30, 2000.
4. Hisada Y. "Evaluation of the input ground motion of the revised seismic code 2000 considering the characteristics of near-source strong ground motions." Architectural Institute of Japan, 2001; **29**: 99-110 (in Japanese).
5. Somerville PG, Smith NF, Graves RW, Abrahamson NA. "Modification of empirical strong ground motion attenuation relations to include the amplitude and duration effects of rupture directivity." Seismological Research Letter, 1997; **68**: 199-222.
6. Stewart JP, Chiou SJ, Bray JD, Graves RW, Somerville PG, Abrahamson NA. "Ground motion evaluation procedures for performance-based design." Pacific Earthquake Engineering Research Center, 2001, PEER Report 2001/09.
7. Rodriguez-Marek A. "Near-fault seismic site response." *Ph.D. Dissertation*, Department of Civil Engineering, University of California, Berkeley, 2000; adviser: Bray JD.
8. Somerville PG. "Development of an improved representation of near fault ground motions." Proceedings of SMIP98 Seminar on Utilization of Strong Motion Data, California Strong Motion Instrumentation Program, Sacramento, CA, USA, 1998; 1-20.
9. Alavi B, Krawinkler H. "Consideration of near-fault ground motion effects in seismic design." Proceedings of the 12th World Conference on Earthquake Engineering, New Zealand 2000.
10. Cox KE, Ashford SA. "Characteristic of a large directivity pulse for laboratory testing." Report no. SSRP-2001/11, Department of Structural Engineering, University of California, San Diego, 2001.
11. Cornell CA. "Engineering seismic risk analysis." Bulletin of Seismological Society of America, 1968; **58**: 1583-1601.
12. Berrill JB. "Building over faults: a procedure for evaluating risk." Earthquake Engineering and Structural Dynamics, 1983; **11**: 427-436.
13. Central Geological Survey, Ministry of Economic Affairs, Taiwan. "Active fault map." 2000 Edition.
14. Loh CH, Huang YJ. "Seismic damage assessment in Taiwan considering characteristic earthquake model." National Center for Research on Earthquake Engineering, Taiwan, 2002, Technical Report no. NCREE-02-032 (in Chinese).
15. Hwang JS, Chiou JM, Sheng LH, Gates JH. "A refined model for based-isolated bridges with bi-linear hysteretic bearings." Earthquake Spectra, 1996; **12**: 245-274.